THE JOURNAL OF FINANCE • VOL. LVIII, NO. 6 • DECEMBER 2003

# What Type of Process Underlies Options? A Simple Robust Test

PETER CARR and LIUREN WU*


## ABSTRACT

We develop a simple robust method to distinguish the presence of continuous and discontinuous components in the price of an asset underlying options. Our method examines the prices of at-the-money and out-of-the-money options as the option's time-to-maturity approaches zero. We show that these prices converge to zero at speeds that depend upon whether the underlying asset price process is purely continuous, purely discontinuous, or a combination of both. We apply the method to S&P 500 index options and find the existence of both a continuous component and a jump component in the index.


To effectively price or hedge derivative securities, or to understand the behavior of financial asset prices in general, it is important to know if they are best modeled using a purely continuous process (PC), a pure jump process (PJ), or a combination of both (CJ). We develop a method to distinguish between these possibilities using options written on the asset in question. Specifically, we examine the market prices of at-the-money (ATM) and out-of-the-money (OTM) options as the option's maturity date approaches the valuation date. While the prices of all ATM and OTM options converge to zero as the time to maturity approaches zero, our theoretical work shows that the speed of convergence differs across the three possibilities (PC, PJ, or CJ). We can thus identify the type of an asset price process by examining the convergence speeds of these option prices.

The simplest approach for determining the type of process governing an asset price is to examine the time series of asset prices directly. However, the discretely sampled paths from the three types of processes look very similar unless the sampling frequency is extremely high. Furthermore, increasing the sampling frequency introduces market microstructure effects. Since our method does not examine the sample path of the underlying asset directly, it circumvents these difficulties.

Our method is able to distinguish the type of process governing the price of an asset because different types of processes have dramatically different implications

* Carr is from Bloomberg LP and the Courant Institute, New York University; Wu is from the Zicklin School of Business, Baruch College, CUNY. The authors thank Rick Green (the editor), an anonymous referee, George Chacko, Xiong Chen, Vladimir Dobric, Robert Engle, John Illuzi, Stewart Inglis, Roger Lee, Keith Lewis, Dilip Madan, Andrew Mitchell, Nate Newlin, Ken Singleton, and participants of the 2002 American Financial Association meetings for helpful comments.

for the prices of short-term options written on that asset. In particular, consider an out-of-the-money option with a very short time to maturity. Under a purely continuous process, the chance that the underlying asset price will move by a large amount over a short interval of time is very small. Hence, the possibility that this out-of-the-money option will move in the money is also very small. In contrast, when the process has jumps, the probability that the underlying asset price can "jump" into the money within any short interval of time is significantly larger. Thus, these two types of processes, although hardly distinguishable from a discretely sampled path, imply rather different behaviors for short-term option prices.

Table I summarizes our theoretical results regarding the speed with which an option's premium approaches zero as the time to maturity $T$ vanishes. We use Landau's notation to characterize the asymptotic speed, so that $f = O(g)$ implies $\limsup(f/g) < \infty$. The table indicates that OTM option prices converge to zero at an exponential rate, $O(e^{-c/T})$, $c > 0$, in the case of a purely continuous sample path, but are dominated by a linear convergence rate, $O(T)$, in the presence of jumps. The table also shows that ATM option prices approach zero at a particular speed, $O(\sqrt{T})$, in the case of a purely continuous sample path. In contrast, ATM option prices can approach zero at a range of speeds in the case of a pure jump process. If the jump process has sample paths with finite variation, for example, a compound Poisson process with a possibly random jump size and potentially time-varying (but finite) jump intensity, the power $p$ in the table is one. However, if the jump process has sample paths of infinite variation and if we can represent the order of convergence by a power function, that power can be anything between zero and one. In the case of a combination of both continuous and discontinuous sample paths, the convergence rate is dominated by the component with the slowest convergence to zero. Thus, observations of the convergence rates of option prices to zero can potentially be used to distinguish the *type* of the process followed by the underlying asset price.

The different decay speeds experienced by option premiums are most easily visualized by a graph. In this paper, we focus on a graph which plots the log of the ratio of option prices to maturity against log maturity. We christen such a graph as a *term decay plot*. The division of option prices by maturity is used to visually contrast order $O(T)$ behavior from sub-$O(T)$ and super-$O(T)$ behavior. For OTM options, the asymptotic behavior of the term decay plots (as the term approaches zero) determines whether or not jumps are being priced into options.

**Table I**
**Asymptotic Behavior of Short-Maturity Options**

| Process Type | OTM Options | ATM Options |
|---|---|---|
| PC | $O(e^{-c/T}), c>0$ | $O(\sqrt{T})$ |
| PJ | $O(T)$ | $O(T^p), p \in (0,1]$ |
| CJ | $O(T)$ | $O(T^p), p \in (0,1/2]$ |

In particular, an asymptotic slope of 0 for the OTM term decay plot implies the existence of a jump component, while an asymptotic slope of positive infinity is consistent with a purely continuous sample path. For ATM options, an asymptotic slope of 0 would imply a pure jump process with finite variation. An asymptotic slope of $-0.5$ implies that either the sample path has a continuous component, or that the jump component exhibits infinite variation or both. An asymptotic slope of any other value implies the existence of an infinite variation pure jump process, which can also be masking a continuous component if the asymptotic slope is below $-0.5$.

The theoretical results in Table I are based on the asymptotic properties of option prices as the option's time to maturity approaches zero. To determine the maturity range at which we can observe the asymptotic behaviors, we simulate several parametric models under each of the three types of processes. For all models simulated, we find that the theoretical asymptotic behavior is always experienced by options maturing within 20 days. In some cases, the asymptotic behavior is experienced over a much longer term. For example, for ATM options in models with a continuous martingale component, the asymptotic behavior is experienced by options maturing within a year. Options with terms from 1 week to 1 year are readily available and liquid for many underlying assets such as stocks, stock indices, currencies, bonds, and so forth. Thus, the types of the sample paths of these assets can readily be tested using market prices of their respective options.

We investigate the process followed by the S&P 500 index by examining the term decay plots on S&P 500 index options at different moneyness levels. From these term decay plots, we conclude that the sample path of the index contains both continuous and discontinuous martingale components. Furthermore, we find that while the presence of the jump component varies strongly over time, the presence of the continuous component is constantly felt. We investigate the implications of the evidence for parametric model specifications.

Our theoretical framework and our proposed method focus on the risk-neutral dynamics of an underlying asset. However, under no arbitrage, the *type* of process found under a risk-neutral measure is preserved under a measure change to the statistical measure. Hence, our findings have implications for both pricing and risk management. More specifically, our findings indicate that risk measurement and management should be conducted under the assumption that the real-world process has both continuous and discontinuous martingale components, with the relative weight of the two components varying over time.

In related work, Aït-Sahalia (2002) introduces the concept of total positivity to finance and shows that the cross second derivative of the transition density of a one-factor diffusion process has to be positive at all states and at all sampling intervals. He constructs a diffusion criterion based on such a property and applies the test to the risk-neutral transition density of the S&P 500 index implied from observed option prices. The test rejects the hypothesis that the index follows a one-factor diffusion process. However, since the test is constructed under the one-factor Markovian setting, his diffusion criterion could also be violated if the index follows a continuous sample path, but is not Markovian in itself. For

example, in the presence of stochastic volatility, the single-factor Markovian property is violated and thus the criterion can be violated even if the asset price follows a continuous sample path. Indeed, the presence of stochastic volatility in asset returns is well documented; see, for example, Bates (1996, 2000), Ding and Granger (1996), Bakshi, Cao, and Chen (1997), and Pan (2002).

Our method presents interesting contrasts to the test proposed by Aït-Sahalia (2002). First, Aït-Sahalia tests whether the underlying asset follows a one-factor Markovian diffusion process or not; our method is designed to identify the presence of a jump component and/or a continuous component and is not confined to a one-factor or Markovian framework. Second, Aït-Sahalia looks at the transition density across *all potential states at any* fixed *time horizon.* In contrast, our method looks at the option price behavior *across maturities at fixed moneyness* (*states*). Hence, the two methods complement each other by focusing on different dimensions of the information set.

The remainder of this paper is organized as follows. The next section develops our theoretical results underlying Table I. Section II simulates popular model candidates under each of three martingale types and analyzes at which maturity options can be characterized by their asymptotic behaviors. Section III applies the procedure to S&P 500 index options. Section IV concludes.

## I. Theory of Short Maturity Option Pricing

### A. Assumptions and Notation

We assume frictionless markets and no arbitrage. Then, under a risk-neutral measure $\mathbb{Q}$, the return on an asset can be modeled as a superposition of a predictable drift component and a martingale. The drift component is determined by no arbitrage. The martingale component can further be decomposed canonically into two orthogonal components: a purely continuous martingale and a purely discontinuous martingale (Jacod and Shiryaev (1987), p. 84).

To fix notation, let $S_t$ denote the spot price of an asset at time $t \in [0, \mathcal{T}]$, where $\mathcal{T}$ is some arbitrarily distant horizon. For simplicity, we assume that the continuously compounded risk-free rate $r$ and dividend yield $q$ are constant. Since we will be looking over short horizons, the time variation of these quantities is not important relative to the martingale components. No arbitrage implies that there exists a risk-neutral probability measure $\mathbb{Q}$ defined on a probability space $(\Omega, \mathcal{F}, \mathbb{Q})$ such that the spot price solves the following stochastic differential equation:

$$dS_t/S_{t-} = (r - q)dt + \sigma_t dW_t + \int_{\mathbb{R}^0} (e^x - 1)[\mu(dx, dt) - \nu_t(x)dxdt], \quad t \in [o, \mathcal{T}] \tag{1}$$

starting at some fixed and known value $S_0 > 0$. In equation (1), $S_{t-}$ denotes the asset price at time $t$ just prior to a jump, $\mathbb{R}^0$ denotes the real line excluding zero, $W_t$ is a $\mathbb{Q}$ standard Brownian motion, and the random measure $\mu(dx, dt)$ counts the number of jumps of size $x$ in the asset price at

time $t$. The process $\{v_t(x),\ x\in\mathbb{R}^0,\ t\in[0,\ \mathcal{T}]\}$, compensates the jump process $J_t \equiv \int_0^t \int_{\mathbb{R}^0} (e^x - 1)\mu(dx, ds)$, so that the last term in equation (1) is the increment of a $\mathbb{Q}$-pure jump martingale.[1] The process $v_t(x)$ is often referred to as the *compensator* or the *local density* of the jumps. Thus, equation (1) models the price change as the sum of a risk-neutral drift and two martingale components: a purely continuous martingale and a purely discontinuous (jump) martingale.

For simplicity, we assume that the jump component in the price process exhibits finite variation:

$$\int_{\mathbb{R}^0} (|x| \wedge 1)v_t(x)dx < \infty, \quad t \in [0, \mathcal{T}], \tag{2}$$

We later relax this assumption and discuss the case of infinite variation jump processes separately. By adding the time subscripts to $\sigma_t$ and $v_t(x)$, we allow both to be stochastic and predictable with respect to the filtration $\mathcal{F}_t$. To satisfy limited liability, we assume the two stochastic processes to be such that the asset price $S_t$ is always nonnegative and absorbing at the origin. We further assume that $\sigma_t$ and $v_t$ are bounded in some neighborhood of $t=0$.

Under our assumption of constant interest rates and dividend yields, the forward price of the asset at time $t$ for some fixed maturity date $T \geq t$ is $F_t = S_t e^{(r-q)(T-t)}$. This forward price is a $\mathbb{Q}$-martingale with the following dynamics:

$$dF_t/F_{t-} = \sigma_t dW_t + \int_{\mathbb{R}^0} (e^x - 1)[\mu(dx, dt) - v_t(x)dxdt], \quad t \in [0, \mathcal{T}], \tag{3}$$

where $F_{t-}$ denotes the prejump forward price at time $t$. We will present our theoretical results in terms of the forward price.

### *B. Time Value Decomposition*

Consider a European call option on an underlying asset with strike price $K$ and maturity $T$. Let time $t=0$ denote the valuation date and let $C_0(K, T)$ denote the time 0 price of the call option. Let $TV_0(K, T)$ denote the call option's *time value*, which is defined as

$$TV_0(K, T) \equiv C_0(K, T) - e^{-rT}(F_0 - K)^+,$$

where $F_0 = S_0 e^{(r-q)T}$ is the time-0 forward price of the asset. The time value of a put option can be defined analogously. Obviously, the option price and time value

[1] We have assumed that the compensator $v(dt, dx)$ of the counting measure has a density given by $v_t(x)$. This compensator must have the following properties (see Prokhorov and Shiryaev (1998)):

$$v(\mathbb{R}^+ \times 0) = 0, \quad v(0 \times \mathbb{R}) = 0, \quad \int_{\mathbb{R}^0} (|x|^2 \wedge 1)v(dt, dx) < \infty, \quad t \in [0, \mathcal{T}].$$

coincide with each other for ATM and OTM options when the moneyness is defined based on forward prices: $K \geq F_0$ for call options and $K \leq F_0$ for put options. Also, put-call parity implies that European put options and call options of the same strike and maturity have the same time value.

The main theoretical result of the paper comes from the following theorem, which decomposes the time value of a European option into two parts: the contribution from the continuous martingale component and that from the purely discontinuous martingale component.

THEOREM 1: *For an asset price process characterized by (1), the time value of a European option on such an asset can be decomposed into two parts*:

$$TV_0(K,T) = e^{-rT}\int_0^T \left[\frac{1}{2}q(K,t)K^2\mathbb{E}_0[\sigma_t^2|F_{t-}=K] + \mathbb{E}_0[F_{t-}v_t^0(k)]\right]dt, \tag{4}$$

*where* $\mathbb{E}_0[\cdot]$ *denotes expectation under the risk-neutral measure* $\mathbb{Q}$ *conditional on filtration* $\mathcal{F}_0$, *q(K, t) denotes the* $\mathbb{Q}$*-probability density function of* $F_{t-}$ *evaluated at* $F_{t-}=K$, *and* $v_t^0(k)$ *is the double tail of the local density defined as,*

$$v_t^0(k) \equiv \begin{cases} \int_k^\infty (e^x - e^k)v_t(x)dx & \text{if } k>0 \\ \frac{1}{2}\int_{\mathbb{R}_0} |e^x-1|v_t(x)dx & \text{if } k=0,\ k\equiv \ln(K/F_{t-}). \\ \int_{-\infty}^k (e^k - e^x)v_t(x)dx & \text{if } k<0 \end{cases} \tag{5}$$

Note that the first part of the time value is related to the quadratic variation of the purely continuous component, while the second part is a function of the compensator of the jump component. Also note that, when $k=0$, the double tail $v_t^0(0)$ is finite only for finite variation jump processes. For $k \neq 0$, $v_t^0(k)$ is finite for all jump types. The proof of the theorem follows from a decomposition of the terminal payoff function via the application of the Meyer-Tanaka formula (see, e.g., Protter (1990), p. 165), which extends Itô's lemma to functions that are not necessarily twice differentiable. We then take expectations to obtain the option value.

*Proof:* We start with a European call option on the asset with strike $K$ and term $T$. The terminal payoff of such an option is given by

$$(S_T - K)^+ = (F_T - K)^+. \tag{6}$$

By the Meyer-Tanaka formula, the terminal payoff function in equation (6) can be decomposed as

$$\begin{aligned}(F_T-K)^+ = (F_0-K)^+ &+ \int_0^T 1(F_{t-}>K)dF_t + \frac{1}{2}\int_0^T F_{t-}^2\sigma_t^2\delta(F_{t-}-K)dt \\ &+\int_0^T\int_{\mathbb{R}^0}[1(F_{t-}\leq K)(F_{t-}e^x-K)^+ + 1(F_{t-}>K)(K-F_{t-}e^x)^+]\mu(dx,dt),\end{aligned} \tag{7}$$

where $\delta(\cdot)$ denotes a *Dirac* delta function. Taking expectations on both sides of equation (7) under measure $\mathbb{Q}$, we have

$$\begin{aligned} e^{rT}C_0(K,T) = (F_0-K)^+ + \frac{1}{2}\int_0^T \mathbb{E}_0[F_{t-}^2\sigma_t^2\delta(F_{t-}-K)]dt \\ + \int_0^T \mathbb{E}_0 \int_{\mathbb{R}^0} [1(F_{t-}\le K)(F_{t-}e^x - K)^+ \\ + 1(F_{t-}>K)(K - F_{t-}e^x)^+]\nu_t(x)dxdt. \end{aligned} \tag{8}$$

Note that the expectation of the second term in equation (7), $\int_0^T 1(F_{t-}>K)dF_t$, is zero by the martingale property of $F_t$. Also note that we replace the random measure $\mu(dx, dt)$ in the jump term by its conditional expected value (compensator) $\nu_t(x)dxdt$ via the law of iterated expectations.

We further factor out $F_{t-}$ from the jump term in equation (8) and represent the term as a function of $k \equiv \ln(K/F_{t-})$, the moneyness of the option just prior to any jump at time $t$. Then, equation (4) follows after the following substitutions and rearrangements:

$$\mathbb{E}_0[F_{t-}^2\sigma_t^2\delta(F_{t-}-K)] = q(K,t)K^2\mathbb{E}_0[\sigma_t^2|F_{t-}=K];$$

$$TV_0(K,T) = C_0(K,T) - e^{-rT}(F_0-K);$$

$$v_t^0(k) = \int_{\mathbb{R}^0}\left[1(k\ge 0)\left(e^x-e^k\right)^+ + 1(k<0)\left(e^k-e^x\right)^+\right]\nu_t(x)dx.$$

Finally, since a European put option has the same time value as a European call option with the same strike and maturity, equation (4) applies to both puts and calls. Q.E.D.

The compensating process $\nu_t(j)$ can be interpreted as the probability per unit time of a jump of size $j$ at time $t$. More precisely,

$$\lim_{\Delta T\downarrow 0}\frac{\mathbb{Q}\{\ln F_{t+\Delta T} - \ln F_{t-}\in dx\}}{\Delta T} \to \nu_t(x)dx, \tag{9}$$

where $\to$ denotes vague convergence on $\{|x|>\varepsilon\}$ for every fixed $\varepsilon>0$ (see Bertoin (1996), p. 39). We label $v_t^0(k)$ as the double tail because it can also be written as the tail of the tail of the local density,

$$v_t^0(k) = \begin{cases} \int_k^\infty e^\ell \int_\ell^\infty \nu_t(x)dxd\ell & \text{if } k>0 \\ \frac{1}{2}\int_0^\infty e^\ell \int_\ell^\infty \nu_t(x)dxd\ell + \frac{1}{2}\int_{-\infty}^0 e^\ell \int_{-\infty}^\ell \nu_t(x)dxd\ell & \text{if } k=0. \\ \int_{-\infty}^k e^\ell \int_{-\infty}^\ell \nu_t(x)dxd\ell & \text{if } k<0 \end{cases}$$

As a corollary, the theorem also tells us the maturity derivative of ATM and OTM options.

COROLLARY 1: *The maturity derivative of an ATM or OTM option can be decomposed into three parts:*

$$\frac{\partial}{\partial T} TV_0(K,T) = e^{-rT}\frac{1}{2}q(K,T)K^2\mathbb{E}_0[\sigma_T^2|F_{T-}=K] + e^{-rT}\mathbb{E}_0[F_{T-}v_T^0(k)] - rTV_0(K,T). \quad (10)$$

When the risk-neutral density $q$ is replaced by the discounted second strike derivative, this expression is often called the forward equation for option prices. Andersen and Andreasen (1999) arrive at a similar result under the assumption of the Poisson jump model of Merton (1976).

### C. Short Maturity Behavior

This section considers the asymptotic behavior of ATM and OTM option prices as their maturity date approaches the valuation date (i.e., $T\downarrow 0$). We first derive the asymptotic behavior based on Theorem 1, under the assumption that the jump component exhibits finite variation. We then consider the special case of infinite variation jump processes.

#### C.1. Continuous Martingale and Finite Variation Jumps

The following proposition is a direct result of Theorem 1.

PROPOSITION 1: *As the time to maturity $T$ approaches zero, option prices converge to zero at rates which depend upon both the moneyness and the type of the underlying price process. OTM option prices converge to zero at the rate of $O(e^{-c/T})$, $c>0$ in the case of a purely continuous process and at the rate of $O(T)$ in the presence of a jump component. ATM option prices converge to zero at the rate of $O(\sqrt{T})$ in the purely continuous case and at the rate of $O(T)$ in the case of a pure jump process with finite variation. The convergence rate is dominated by the lower order of the two when both components are present.*

*Proof:* As $T\downarrow 0$, equation (4) implies that the time value of an option can be approximated as

$$TV_0(K,T) \sim T\left[\frac{1}{2}q(K,T)K^2\ell_0^2(K) + F_0 v_0^o(k)\right], \quad (11)$$

where $f\sim g$ implies $\lim(f/g)=1$ and $\ell_0^2(K)\equiv\mathbb{E}_0(\sigma_T^2|F_{T-}=K)$ as $T\downarrow 0$. We drop the interest rate discounting term $e^{-rT}$ because it converges to one as $T\downarrow 0$. We also drop the expectation operation on $v_t^0$, given that it is predictable with respect to the filtration $\mathcal{F}_t$. Finally, we replace $\mathbb{E}_0[F_{T-}|F_0]$ with $F_0$ as $T\downarrow 0$.

We first consider OTM options ($K\neq F_0$). In the case of a purely continuous process ($v_0^o=0$), the time value reduces to

$$TV_0(K,T) \sim T\frac{1}{2}q(K,T)K^2\ell_0^2(K).$$

Hence, the order of decay depends on the density function $q(K, T)$. But as $T \downarrow 0$, all continuous processes behave like a standard Brownian motion (for the diffusion case, see Varadhan (1967)). The probability density function approaches the following Gaussian density:

$$q(K,T) \sim \frac{1}{\sqrt{2\pi T}F_0\ell_0(K)} \exp\left(-\frac{(F_0-K)^2}{2F_0^2\ell_0^2(K)T}\right), \quad K \neq F_0.$$

Therefore, asymptotically, the time value decays at an exponential rate in this purely continuous case,

$$TV_0(K,T) \sim \frac{\sqrt{T}K^2\ell_0(K)}{2\sqrt{2\pi}F_0} \exp\left(-\frac{(F_0-K)^2}{2F_0^2\ell_0^2(K)T}\right) \sim \sqrt{T}O(e^{-c/T}), c>0, \qquad (12)$$

where $O(\cdot)$ denotes the order of the decay in terms of maturity. In the case of a pure jump process ($\sigma^2 = 0$), the time value reduces to

$$TV_0(K,T) \sim TF_0v_0^o(k) \sim O(T).$$

In the case of both a continuous and a jump component, the decay rate is dominated by that of the jump component, $O(T)$.

For ATM options ($K = F_0$), the time value formula in equation (11) still holds. But the probability density function $q(K, T)$ is reduced to[2]

$$q(K,F) \sim \frac{1}{\sqrt{2\pi T}F_0\ell_0(K)}, \quad K = F_0.$$

The decay rate implied by a purely continuous process is therefore $O(\sqrt{T})$. In the case of a pure finite variation jump process, the asymptotic rate of $O(T)$ still holds. Q.E.D.

### *C.2. Infinite Variation Jump Processes*

Theorem 1 and hence Proposition 1 are derived under the assumption that the jump martingale component, if it is present, exhibits sample paths of finite variation. In particular, the at-the-money double tail $v_t^o(0)$ in equation (5) is finite only under the assumption (2) of finite variation sample paths. The following proposition considers the asymptotic behavior of option prices when the underlying asset price process follows a pure jump process whose sample paths have infinite variation.

PROPOSITION 2: *Suppose that the underlying asset price process is driven by a pure jump martingale with sample paths of infinite variation. Then, as the maturity date approaches the valuation date, ATM option prices can converge to zero at a range of speeds. If we assume that the dependence of option price on maturity is $O(T^p)$, then*

[2] Brenner and Subrahmanyam (1988) derive a similar result under the Black–Scholes setting.

*the order is $p \in (0,1)$. OTM option prices converge to zero at the rate of $O(T)$, the same as the case with finite variation jump processes.*

Table I summarizes the results in Propositions 1 and 2.

*Proof:* For OTM options, that is, for moneyness $k \equiv \ln(K/F_0) \neq 0$, the double tail $v_0^o(k)$ in (5) is well defined even if the jump process exhibits infinite variation. Thus, the order $O(T)$ decay rate for finite variation jump processes proved in Proposition 1 extends to infinite variation jump processes.

For ATM options, the double tail $v_t^o(0)$ in (5) is not well defined for jump processes with infinite variation. For such processes, we define the ATM double tail $v_t^o(0)$ as

$$v_t^o(0) = \frac{1}{2}\int_{\mathbb{R}^0} |e^x - 1 - x1_{|x|<1}| v_t(x)dx, \tag{13}$$

where the truncation is needed to keep the double tail finite. But the truncated small jumps also induce a different order of time dependence. In particular,

$$\lim_{T\downarrow 0}\int_0^T \mathbb{E}_0 \int_{|x|<1} |x| v_t(x)dxdt = \lim_{T\downarrow 0}\int_{|x|<1} |x| \mathbb{Q}\{\Delta \ln F_{t\in(0,T]} \in dx\}, \tag{14}$$

where $\Delta \ln F_{t\in(0,T]}$ denotes the jumps in $\ln F$ during the period $t \in (0, T]$. Suppose we assume that $\lim_{T\downarrow 0}\int_{|x|<1} |x| \mathbb{Q}\{\Delta \ln F_{t\in(0,T]} \in dx\} \sim O(T^p)$. The fact that $\int_{|x|<1} |x| v(x)dx = \infty$ for infinite variation jumps implies the order $p$ is smaller than one. The requirement that time value increases with maturity demands that the order $p$ be positive and, hence, $p \in (0, 1)$. The $O(T^p)$ decay rate induced by the small jumps dominates the $O(T)$ decay rate induced by large jumps for ATM options. Q.E.D.

The behavior of infinite variation jump martingales can be further illustrated via the classical example of an $\alpha$-stable Lévy motion. In particular, the finite moment log stable (LS) model of Carr and Wu (2003a) uses the $\alpha$-stable Lévy motion with maximum negative skewness as the martingale component of the risk-neutral process for asset prices:

$$S_t = S_0 e^{(r-q)t + \sigma^\alpha \sec\frac{\pi\alpha}{2} t + \sigma L_t^{\alpha,-1}}, \quad t \in [0, T], \alpha \in (1,2), \sigma > 0, \tag{15}$$

where the $\alpha$-stable Lévy motion $L_t^{\alpha,\beta}$ has an $\alpha$-stable distribution with zero drift, dispersion of $t^{1/\alpha}$, and a skewness parameter $\beta$. Setting $\beta = -1$ in the LS model guarantees the existence of a martingale measure and the finiteness of call option values. The term $\mu = \sigma^\alpha \sec(\pi\alpha/2)$ in equation (15) denotes the convexity adjustment term, which is finite only when the $\alpha$-stable motion exhibits maximum negative skewness.

A key feature of the $\alpha$-stable Lévy motion is its *self-similar* property: $L_t^{\alpha,\beta}$ and $t^{1/\alpha} L_1^{\alpha,\beta}$ possess the same distribution. Based on this property, we prove the following asymptotic behavior for ATM options under the LS model.[3]

[3] We thank Xiong Chen for much of this proposition.

PROPOSITION 3: *Under the LS model in (15), ATM option prices converge to zero at the rate of* $O(T^{1/\alpha})$.

*Proof:* Based on (15), the forward price $F_T$ is an exponential martingale,

$$F_T = F_0 e^{\mu T + \sigma L_T^{\alpha,-1}} = F_0 e^{\mu T + \sigma T^{1/\alpha} L_1^{\alpha,-1}}.$$

The second equality is obtained by the self-similar property of the $\alpha$-stable Lévy motion.

Now consider the value of an ATM call option ($K = F_0$),

$$\begin{aligned} TV_0(F_0, T) &= \mathbb{E}_0\left[(F_T - F_0)^+\right] = F_0 \mathbb{E}_0\left[\left(e^{\mu T + \sigma T^{1/\alpha} L_1^{\alpha,-1}} - 1\right)^+\right] \\ &= F_0 \int_{-\frac{\mu}{\sigma} T^{1-1/\alpha}}^{\infty} \left(e^{\mu T + \sigma T^{1/\alpha} x} - 1\right) q(x) dx, \end{aligned}$$

where $q(x)$ denotes the probability density function of a standardized $\alpha$-stable random variable with zero mean and unit dispersion.

By Taylor expansion, one can show that

$$\lim_{T \downarrow 0} \frac{\exp(\mu T + \sigma T^{1/\alpha} x) - 1}{T^{1/\alpha}} \to \sigma x.$$

Hence,

$$\lim_{T \downarrow 0} \frac{TV_0(F_0, T)}{T^{1/\alpha}} \to F_0 \sigma \int_0^{\infty} x q(x) dx < \infty.$$

Therefore, ATM option prices converge to zero at the rate of $O(T^{1/\alpha})$. Q.E.D.

An $\alpha$-stable Lévy motion is fully characterized by its Lévy measure,

$$v(x) = c_{\pm} x^{-\alpha - 1}, \tag{16}$$

where $c_+$ and $c_-$ apply to the cases of $x > 0$ and $x < 0$, respectively. The maximum negative skewness in the LS model is achieved by setting $c_+ = 0$ and, hence, by only allowing negative jumps. The admissible domain of the tail index $\alpha$ for an $\alpha$-stable motion is $\alpha \in (0, 2]$. The LS model restricts that $\alpha > 1$ so that the return has the support of the whole real line. An $\alpha$-stable Lévy motion exhibits infinite variation when $\alpha > 1$ because the following integral is not finite:

$$\int_{\mathbb{R}^0} (|x| \wedge 1) x^{-\alpha - 1} dx = \infty.$$

Nevertheless, to maintain finite quadratic variation, that is,

$$\int_{\mathbb{R}^0} (|x|^2 \wedge 1) x^{-\alpha - 1} dx < \infty,$$

the tail index $\alpha$ cannot be greater than two. Therefore, the LS model can generate a range of convergence speeds for ATM options, $O(T^p)$, for $p \in (1/2, 1)$. As $\alpha$

approaches two, the $\alpha$-stable Lévy motion degenerates into a (continuous) Brownian motion and the asymptotic decay rate approaches $O(\sqrt{T})$.

We thus obtain very different behaviors for the short-term values of options as we vary the *type* of the underlying asset price process. For OTM options, as the maturity date approaches the valuation date, the decay rate of the jump component, $O(T)$, dominates the decay rate of the continuous martingale component, $O(e^{-c/T})$, $c>0$, since for small $T$, $e^{-c/T} << T$. Thus, should the decay rate of OTM option values be $O(T)$, we can conclude that there exists a jump component in the underlying asset price dynamics. We can then determine the existence of an infinite variation component (a continuous process or infinite variation jump process) from the short maturity behavior of ATM options. If the observed decay rate for ATM options is also $O(T)$, we can conclude that the underlying process is a pure jump process with finite variation. On the other hand, if the observed decay rate is of order $O(\sqrt{T})$, there may exist a continuous martingale component and/or a jump component with infinite variation.

Now, suppose that the actual behavior of the underlying asset price has a jump component, and that market makers price options by inserting an implied volatility into the pure diffusion Black–Scholes formula. The assumption that the actual price process has jump components implies that the OTM option values decay as $O(T)$. From equation (12), we see that for OTM option values to decay at this rate, the implied volatility must approach infinity at rate $\sqrt{T}O(e^{c/T}), c>0$ as $T\downarrow 0$. The fact that market makers often abandon the use of implied volatility for OTM options at short maturities suggests that jumps are priced into options at short maturities. Our empirical work in Section III confirms this conjecture.

This last point also brings us back to one of our assumptions. Although we allow $\sigma_t$ and $v_t$ to be stochastic, we do assume that they are bounded in a neighborhood of $t=0$. Hence, the leading term in the time expansion is of order zero. As a counter example, suppose that we modify the Black–Scholes model by allowing the volatility to vary deterministically over time at the rate $\sqrt{T}O(e^{c/T}), c>0$. Then, the OTM option values would decay as $O(T)$ even though the underlying price process is a purely continuous process. However, the explosive nature of models like this excludes themselves from our consideration.

## II. Simulation of Popular Models

The different asymptotic behaviors for ATM and OTM options under different models can be best captured by a graph of $\ln(P/T)$ versus $\ln(T)$, where $P$ denotes the prices of ATM or OTM options and $T$ denotes the option term. We christen this graph as a *term decay plot*. Propositions 1 and 2 imply that as the option maturity approaches the valuation date, the term decay plot for ATM options exhibits either (1) a flat line in the case of a finite variation pure jump model or (2) a downward sloping straight line in the presence of a continuous martingale component or an infinite variation jump component. On the other hand, a similar plot for

OTM options exhibits either (1) a flat line in the presence of jumps or (2) an upward sloping concave curve in the case of a purely continuous process.

In this section, we simulate the behavior of several popular models under each of the martingale types. We focus on when the asymptotic behavior of options will become transparent from the term decay plot. Since we intend to apply the method to the S&P 500 index options market, the parameters of each simulated model are chosen to approximate the behavior of S&P 500 index options. In all of the simulation analysis, we set the interest rate and dividend yield constant at the empirically determined averages of $r = 5.96\%$ and $q = 1.31\%$.[4] We focus on the behavior of OTM and ATM put values because in practice OTM put options are more liquid than OTM calls in the S&P 500 index options market. For each model, we compute put option prices at four moneyness levels: $k = \ln(K/F) = 0$, $-3.07\%$, $-6.14\%$, and $-9.20\%$, and at a range of maturities: $\ln T = [-4, 0]$ with an equal interval of 0.2. This maturity range corresponds to option maturities from 5 business days to 1 year. We analyze the term decay plots over this maturity range at each of the four moneyness levels. In particular, to assess the slope and curvature of these term decay plots,[5] we perform a second-order polynomial fit to the plots:

$$\ln(P/T) = a(\ln T)^2 + b(\ln T) + c.$$

Then, the slope of the plot at a certain maturity $T$ is given by $2a\ln(T) + b$ and the curvature is given by $2a$. Table II reports the slope and curvature estimates of the term decay plots for all simulated models. To save space, we only report the estimates on term decay plots at moneyness $k = 0$ and $k = -9.20\%$. The slopes are measured at the short end of the maturity: $\ln T = -4$. The second-order polynomial fits the simulated term decay plots well, with $R$-squares for all simulated plots greater than 0.97.

### *A. Purely Continuous Processes*

We consider two candidates for purely continuous processes: One is the classic Black and Scholes (1973) model; the other is its stochastic volatility extension by Heston (1993). The Black–Scholes model leads to a geometric Brownian motion for the stock price under the risk-neutral measure $\mathbb{Q}$,

$$dS_t = (r - q)S_t dt + \sigma S_t dW_t,$$

with constant instantaneous volatility $\sigma$. The Heston model allows the volatility to be stochastic and assumes that the instantaneous variance rate $v = \sigma^2$ follows a mean-reverting square-root process under measure $\mathbb{Q}$,

$$dv_t = \kappa(\theta - v_t)dt + \sqrt{\beta v_t}dZ_t, \tag{17}$$

[4] While choosing an interest rate and dividend yield close to data average mimics better the behavior of the S&P 500 index options, our experiment shows that setting both to zero generates almost the same qualitative shape for the term decay plots.

[5] We thank the referee for pointing out that the curvature of the term decay plot also contains valuable information.

**Table II**

**Slope and Curvature of Simulated Term Decay Plots**

Entries report the slope and curvature estimates (standard errors in parentheses) from simulated term decay plots based on a second-order polynomial fit:

$$\ln(P/T) = a(\ln T)^2 + b(\ln T) + c,$$

where $P$ and $T$ denote, respectively, the put option price and the maturity of the option. The polynomial fitting is performed on simulated prices at the log maturity range of $\ln T = [-4{:}0]$, with an equal interval of 0.2. Based on the estimates for the polynomial coefficients $[a, b]$, the slope of the curve is $2a \ln T + b$ and the curvature, $2a$. We evaluate the slope at the short end of the maturity: $\ln T = -4$. Also reported is the $R^2$ of each polynomial fitting.

| | $\ln K/F = 0$ | | | $\ln K/F = -9.2\%$ | | |
|---|---|---|---|---|---|---|
| Model | Slope | Curvature | $R^2$ | Slope | Curvature | $R^2$ |
| | | | *A. Pure Continuous Models* | | | |
| BS | −0.497 | −0.003 | 1.000 | 1.988 | −0.713 | 0.976 |
| | (0.000) | (0.000) | – | (0.092) | (0.044) | – |
| Heston | −0.493 | −0.018 | 1.000 | 3.158 | −1.092 | 0.979 |
| | (0.001) | (0.000) | – | (0.142) | (0.069) | – |
| | | | *B. Pure Jump Models* | | | |
| MJ | 0.086 | −0.155 | 0.997 | 0.027 | −0.096 | 0.999 |
| | (0.012) | (0.006) | – | (0.004) | (0.002) | – |
| LS | −0.357 | −0.017 | 1.000 | 0.085 | −0.068 | 0.973 |
| | (0.001) | (0.000) | – | (0.009) | (0.004) | – |
| LS (α) | | | *C. Impact of Tail Index under LS Model* | | | |
| 1.2 | −0.241 | −0.034 | 1.000 | 0.044 | −0.068 | 0.997 |
| | (0.001) | (0.001) | – | (0.004) | (0.002) | – |
| 1.5 | −0.357 | −0.017 | 1.000 | 0.085 | −0.068 | 0.973 |
| | (0.001) | (0.000) | – | (0.009) | (0.004) | – |
| 1.9 | −0.474 | −0.005 | 1.000 | 0.605 | −0.170 | 0.973 |
| | (0.001) | (0.000) | – | (0.040) | (0.019) | – |
| 2.0 | −0.498 | −0.003 | 1. 000 | 3.255 | −1.098 | 0.980 |
| | (0.000) | (0.000) | – | (0.149) | (0.072) | – |
| | | | *D. Mixture Models* | | | |
| MJD | −0.347 | −0.019 | 1.000 | 0.042 | −0.065 | 0.993 |
| | (0.005) | (0.002) | – | (0.007) | (0.003) | – |
| LSD | −0.452 | −0.005 | 1.000 | 0.369 | −0.163 | 0.972 |
| | (0.001) | (0.000) | – | (0.014) | (0.007) | – |

where $Z_t$ is another standard Brownian motion with $\mathbb{E}[dW_t dZ_t] = \rho dt$. The option pricing formula for the Black–Scholes model is well known. Option prices under the Heston model can be efficiently computed via the FFT method of Carr and Madan (1999), given the characteristic function of the log price relative $s_T = \ln(S_T/S_0)$,

$$\phi(u) \equiv \mathbb{E}_0[e^{ius_T}] = \exp[iu(r-q)T - b(T)v_0 - c(T)],$$

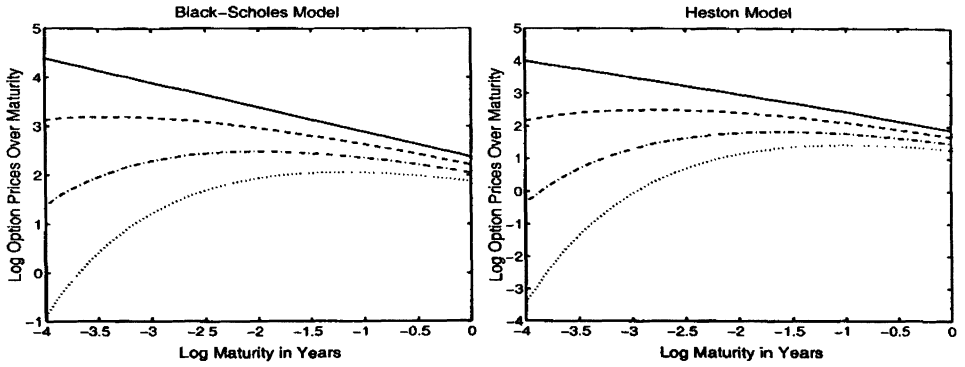


**Figure 1. The term decay plots under purely continuous processes.** Lines are log put option prices over maturity plotted against log maturity. Option prices are computed from, in the left panel, the Black–Scholes model with $\sigma = 27.4\%$ and, in the right panel, the Heston model with $\theta = 0.0348$, $\kappa = 1.15$, $\beta = 0.1521$, $\rho = -0.64$, $v_0 = \theta$. We further assume spot price $S = 100$, interest rate $r = 5.96\%$, and dividend yield $q = 1.31\%$. In each panel, the moneyness $k = \ln(K/F)$ is, from top to bottom, 0 (solid line), $-3.07\%$ (dashed line), $-6.14\%$ (dash-dotted line), and $-9.20\%$ (dotted line).

where $v_0$ is the current level of the instantaneous variance rate and the coefficients $\{b(T), c(T)\}$ are the following functions of term $T$:

$$b(T) = \frac{2\delta(1 - e^{-\eta T})}{2\eta - (\eta - \kappa*)(1 - e^{-\eta T})};$$

$$c(T) = \frac{\kappa\theta}{\beta}\left[2\ln\left(1 - \frac{\eta - \kappa*}{2\eta}(1 - e^{-\eta T})\right) + (\eta - \kappa*)T\right],$$

with

$$\eta = \sqrt{(\kappa*)^2 + 2\beta\delta}, \quad \kappa* = \kappa - iu\sqrt{\beta}\rho, \quad \delta = (iu + u^2)/2 \cdot$$

Figure 1 depicts the term decay plots under the two PC models. The volatility, $\sigma$, in the Black–Scholes model is set to 27.4%, a number close to the average of the implied volatility quotes on S&P 500 index options in our sample period. The parameters for the Heston model are adopted from the estimates in Bakshi et al. (1997), who also calibrate the model to S&P 500 index options. The term decay plots of the two PC models exhibit very similar behaviors. In particular, the plots for ATM options look like straight lines for both models as the term varies from 5 days to 1 year. Panel A of Table II reports the slope and curvature estimates of these term decay plots. The plots for ATM options show very little curvature ($-0.003$ and $-0.018$) for the two PC models, and their short-maturity slope estimates ($-0.497$ and $-0.493$) are close to the asymptotic theoretical value of $-0.5$. Thus, for purely continuous processes, regardless of whether stochastic volatility is present or not, the term decay plot for ATM options converges to its asymptotic

behavior of a straight line at relatively long and hence readily observable maturities.

On the other hand, the term decay plots for OTM options are all upward sloping and concave, as expected from the asymptotic decay rate of $O(e^{-1/T})$ for continuous models. This behavior, particularly the upward sloping curve at short maturities, is more obvious for options deeper out of the money. The estimates in Table II confirm this observation. At moneyness $\ln(K/F) = -9.2\%$, the term decay plots for both PC model exhibit strong concavity, with curvature estimates at $-0.713$ and $-1.092$. Furthermore, the short-maturity slope estimates are large and positive, 1.988 for the Black–Scholes model and 3.158 for the Heston model.

### *B. Pure Jump Processes*

Under pure jump processes, OTM options converge to zero at the rate of $O(T)$ as time to maturity approaches zero. Hence, the term decay plot should converge to a flat line at short maturities. In contrast, the decay rate of ATM options depends upon whether the sample path of the jump process exhibits finite or infinite variation. In this subsection, we simulate two pure jump models, one with finite variation and the other with infinite variation. For the finite variation jump type, we simulate the most popular jump model, the compound Poisson jump model of Merton (1976) (MJ). While we recognize that MJ is usually implemented with a diffusion component, we investigate here the behavior of the pure jump version of his model. Under MJ, the arrival rate of jumps is controlled by a Poisson distribution with a constant and finite intensity $\lambda$. Conditional on one jump occurring, we assume that the size of the jump in the log price is drawn from a normal distribution with mean $\mu_j$ and variance $\sigma_j^2$. For the infinite variation jump type, we simulate the log stable (LS) model of Carr and Wu (2003a) as described in equation (15). The driver of the process is an $\alpha$-stable Lévy motion with maximum negative skewness. The characteristic functions of the log returns under the two pure jump models are

$$\phi_{MJ}(u) = \exp\left[iu\left(r - q - \lambda\left(e^{\mu_j + \frac{1}{2}\sigma_j^2} - 1\right)\right)T + \lambda\left(e^{iu\mu_j - \frac{1}{2}u^2\sigma_j^2} - 1\right)T\right];$$

$$\phi_{LS}(u) = \exp\left[iu\left(r - q + \sigma^2 \sec\frac{\pi\alpha}{2}\right)T - T(iu\sigma)^\alpha \sec\frac{\pi\alpha}{2}\right].$$

Figure 2 depicts the term decay plots implied by the two pure jump models at four different moneyness levels. Parameters are chosen to fit the general features of the S&P 500 index options.[6] The term decay plots for OTM options are similar under both jump types and converge to their asymptotic behavior of a flat line as maturity falls within a month. As shown under Panel B of Table II, for OTM options with moneyness $\ln(K/F) = -9.2\%$, the short-maturity slope estimates for the term decay plots under both models are close to the asymptotic value of zero: 0.027 for MJ and 0.085 for LS. The two plots also exhibit little curvature: $-0.096$ for MJ and $-0.068$ for LS.

[6] The parameters are adopted (but rounded off) from estimates in Carr and Wu (2003a).

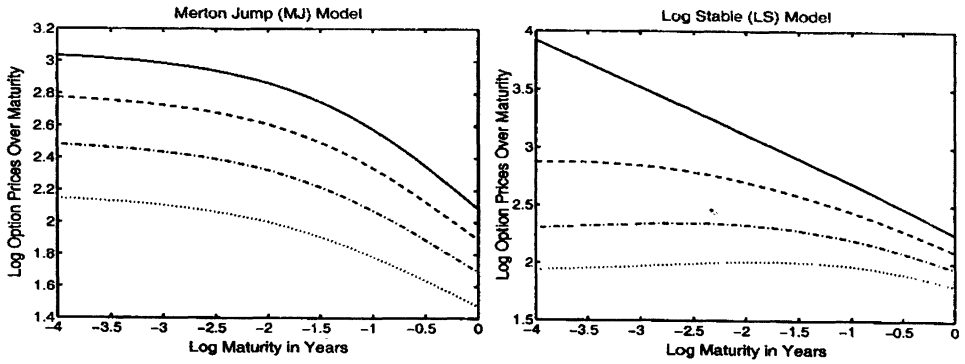


**Figure 2. The term decay plots under purely discontinuous processes.** Lines are log put option prices over maturity plotted against log maturity. Option prices are implied by the MJ model in the left panel and the LS model in the right panel. The model parameters are set to $\lambda = 2$, $\mu_j = -0.10$, $\sigma_j = 0.13$ for MJ and $\sigma = 0.15$, $\alpha = 1.5$ for LS. We further assume spot price $S = 100$, interest rate $r = 5.96\%$, and dividend yield $q = 1.31\%$. In each panel, the moneyness $k = \ln(K/F)$ is, from top to bottom, 0 (solid line), $-3.07\%$ (dashed line), $-6.14\%$ (dash-dotted line), and $-9.20\%$ (dotted line).

In contrast, the term decay plots for ATM options exhibit distinct behaviors under the two types of pure jump processes. Under the finite variation MJ model, the ATM term decay plot flattens out as maturity falls within a month, similar to that for OTM options. The plot exhibits small concavity, with a curvature estimate of $-0.155$, and the short-maturity slope estimate is 0.086, very close to zero. On the other hand, under the infinite variation LS model, the ATM term decay plot cannot be visually distinguished from a straight line, similar to the behavior of a purely continuous process. The curvature estimate is very close to zero at $-0.017$, and the short-maturity slope estimate is $-0.357$, much closer to the asymptotic rate of a continuous component ($-0.5$), than to the asymptotic rate of finite variation jumps (0). According to Proposition 3, under the LS model, the theoretical asymptotic decay rate for the ATM term decay plot is $1/\alpha - 1$. Given that we set $\alpha = 1.5$, the theoretical asymptotic rate is $-0.333$.

While one can easily distinguish the ATM option behavior implied by a purely continuous process from a pure jump process with finite variation, the differences are not as easily discerned if the jump process also exhibits infinite variation. Furthermore, the infinite variation pure jump LS model degenerates into a pure diffusion model (the Black–Scholes model) as the tail index $\alpha$ approaches two. Figure 3 further illustrates how, under the LS model, the behaviors of ATM and OTM option prices change at different values for the tail index $\alpha$. As shown in the left panel, all the plots for the ATM options look like straight lines: The curvature estimates are all close to zero. Furthermore, the short-maturity slope estimates, as reported in Panel C of Table II, become closer to the asymptotic value of $-0.5$ of a continuous martingale as the tail index approaches two: The estimates are $-0.241$, $-0.357$, $-0.474$, and $-0.498$ for $\alpha = 1.2, 1.5, 1.9, 2.0$, respectively. The corresponding theoretical asymptotic values are, respectively, $-0.167$, $-0.333$, $-0.474$, and $-0.5$.

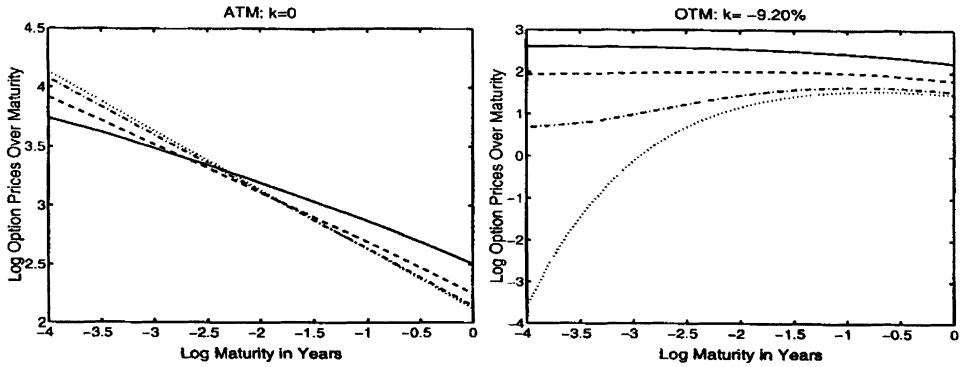


**Figure 3. The behavior of option prices under the LS model.** Lines are log put option prices over maturity plotted against log maturity under the LS model with $S=100$, $r=5.96\%$, $q=1.31\%$, $\sigma=15\%$, and $\alpha$ equals, respectively, 1.2 (solid line), 1.5 (dashed line), 1.9 (dash-dotted line), and 2.0 (dotted line). The moneyness $k=\ln(K/F)$ is 0 (ATM) in the left panel and $-9.20\%$ in the right panel.

For OTM options ($k=-9.20\%$, right panel in Figure 3), the distinction between a continuous ($\alpha=2$, dotted line) and a jump ($\alpha<2$) process looks more obvious. The short-maturity slope estimates are small at 0.044, 0.085, and 0.605 for $\alpha=1.2, 1.5, 1.9$, but increase to 3.255 as $\alpha=2$. Similarly, the curvature estimates of the plots are also small ($-0.068$, $-0.068$, and $-0.170$) when $\alpha<2$ but are much larger ($-1.098$) when $\alpha=2$. When $\alpha$ increases from 1.9 to 2.0, the behaviors of the OTM options change dramatically.

### *C. Combined Continuous-Jump Processes*

To each of the two pure jump models (MJ and LS) with parameters in Figure 2, we add a continuous (diffusion) component with a constant instantaneous volatility of 14%, which is about half the average of the implied volatility quotes. The behavior of the combined models (MJD and LSD) is illustrated in Figure 4. The dominance of the diffusion component on the short maturity behavior of the ATM options is obvious, especially for models with finite variation jumps. For both models, the term decay plots for ATM options look more or less like straight lines. The curvature estimates of the ATM term decay plots for both models are close to zero: $-0.019$ for MJD and $-0.005$ for LSD (Panel D, Table II). Nevertheless, the short-maturity slope estimates for the plots are both smaller in absolute values than the asymptotic slope of the diffusion component ($-0.5$). They are $-0.347$ for the MJD model and $-0.452$ for the LSD model. Hence, although the diffusion component is more dominating in the behavior of ATM options, the role of the jump component is still visible.

As the short maturity behavior of the OTM options is dominated by the jump component, the term decay plots for OTM options are very similar to those observed in Figure 2. The slope and curvature estimates of the plots for the MJ model and the MJD model are very close. Nevertheless, the diffusion component

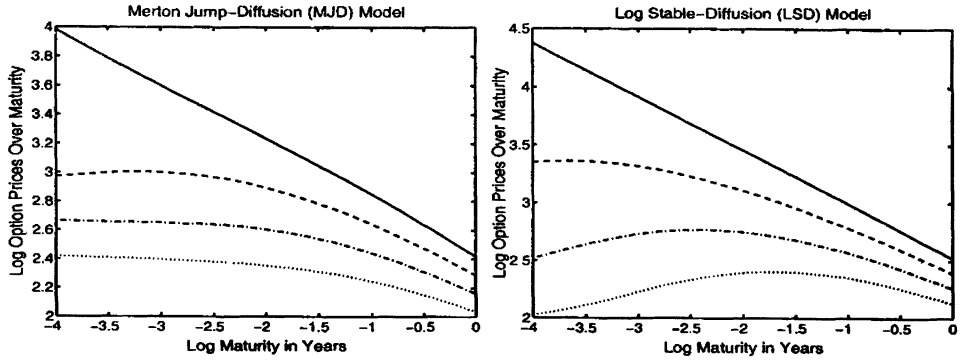


**Figure 4. Term decay plots under mixture models.** Lines are log put option prices over maturity plotted against log maturity. Option prices are implied by a mixture of a diffusion component with a constant instantaneous volatility of 14% and a jump component. The jump component is MJ in the left panel and LS in the right panel with parameters the same as in Figure 2. In each panel, the moneyness $k = \ln(K/F)$ is, from top to bottom, 0 (solid line), $-3.07\%$ (dashed line), $-6.14\%$ (dash-dotted line), and $-9.20\%$ (dotted line).

seems to have a visible impact on the OTM term decay plots under the LSD model. Under moneyness $\ln(K/F) = -9.2\%$, incorporating a diffusion component makes the short maturity slope estimate slightly more positive from 0.085 for LS to 0.369 for LSD, and makes the curvature estimate slightly more negative from $-0.068$ for LS to $-0.163$ for LSD. Furthermore, simulation exercises (not reported) also indicate that the exact shape of the term decay plots are also affected by the relative magnitude of the two components.

In summary, as time to maturity approaches zero for OTM options, their price behavior is dominated by the presence of a jump component. This asymptotic dominance can be visually identified from options with maturities of 20 days or less. Thus, we can readily identify the presence of jumps in the underlying asset price movement from the short maturity behavior of OTM option prices. In addition, the short maturity behavior of the ATM options provides further information on the existence of an infinite variation component (from either a continuous or discontinuous process). The asymptotic dominance of this component on the behavior of ATM options becomes apparent as the option maturity falls within one year.

## III. The Term Decay Plots for S&P 500 Index Options

We now turn to analyzing the behavior of the term decay plots for S&P 500 index options, from which we infer the type of process the index follows.

### *A. Data and Estimation*

The data on S&P 500 index options are obtained from a major bank in New York City. The data set contains daily closing bid and ask price and implied

volatility quotes on out-of-the-money options on the cash (i.e., spot value of the) S&P 500 index across all strikes, $K$, and maturities, $T$, from April 6, 1999 to May 31, 2000 (290 business days). These index options are listed at the Chicago Board of Options Exchange (CBOE). The data set also includes the matching forward prices $F$, spot index levels $S$, and interest rates $r$ corresponding to each option quote. We apply the following filters to the data: (1) the time to maturity is greater than 5 business days, (2) the bid option price is strictly positive, and (3) the ask price is no less than the bid price. After applying these filters, we also plot the implied volatility midquote for each day and maturity against strike prices to visually check for obvious outliers. After removing these outliers, we have 62,950 option quotes left over a period of 290 business days. From this data set, we construct term decay plots for S&P 500 index options and investigate the type of process underlying this index.

We filter out very short maturities contracts and zero-bid contracts to minimize the impact of microstructure effects on the quotes. Our visual plot-by-plot inspection further removes the potential impact of data outliers. A potential concern of short maturity options is nonsynchronicity between option quotes and the underlying index levels. This issue is partially removed in our data set as the bank also provides a matching implied volatility quote for each option, which, in general, does not vary as much with the underlying spot level as the option price does. In converting implied volatilities to option prices, we further normalize the option price as percentages of the underlying forward price. This normalization makes the term decay plots less sensitive to the underlying price movement, thus facilitating intertemporal comparison.

For ease of comparison with the simulated models, we construct the term decay plots for S&P 500 index options under the same moneyness levels as those in the simulation plots (Figures 1 to 4): $k = \ln(K/F) = 0$, $-3.07\%$, $-6.14\%$, and $-9.20\%$. However, the observed option quotes do not always correspond to these moneyness levels. In particular, since the forward price $F$ is varying every day while the strike prices $K$ are fixed, the moneyness levels $k = \ln(K/F)$ are varying over time. Thus, we need to interpolate across strike prices to obtain option prices at these fixed moneyness levels. For the interpolation to work with sufficient precision, we require that at each day and maturity, we have at least five option quotes. We do not extrapolate. Visual inspection indicates that at each date and maturity, the quotes are so close to each other along the moneyness line that interpolation can be done with little error, irrespective of the interpolation method. For the reported results, we use spline interpolation on put option prices across moneyness $k$ at each maturity and date. We have also experimented with several different interpolation schemes and on different spaces. The results are almost identical.

Given the interpolated option prices at each fixed moneyness level, we construct a smoothed term decay plot at each of the four fixed moneyness at each date by fitting a simple second-order polynomial function,

$$\ln(P/T) = a(\ln T)^2 + b(\ln T) + c,$$

with $P$ being the put option price (midquote) as a percentage of the underlying forward price and $T$ being the maturity. As discussed in the simulation section, this second-order polynomial regression fits the simulated term decay plots very well and provides a convenient way of summarizing the slope and curvature information of the term decay plots. To estimate the smoothed term decay plot on the real data, we further require that there are at least five distinct maturities at each date and drop those days with smaller cross sections. Of the whole sample, 284 days satisfy this criterion.

Since the second-order polynomial regression fits all the simulated term decay plots very well, the goodness-of-fit on the real data provides another criterion on the quality, and synchronicity in particular, of the data. We would have more confidence on the quality of the data if the data points mostly lie on a smooth second-order polynomial curve. We find that, on most days, the second-order polynomial fits the data well. The average $R$-square for all of the fittings is 0.98. Nevertheless, visual inspection identifies a few days when some maturities deviate significantly from a smoothed term decay curve. The $R$-squares at these days are low as a result. We suspect that these days are more likely to have data measurement errors. We hence use the $R$-squares as yet another criterion to filter the data: We drop any days when any one of the four polynomial regressions (at different moneyness levels) has an $R$-squared less than 0.80. Finally, we have 273 days left, with an average $R^2$ of 0.99. After applying all of our filters, we believe that the impact of microstructure effects on our analysis is minimal. Armed with these smoothed term decay plots, we analyze the underlying process followed by the S&P 500 index.

### *B. Is There a Jump Component?*

The key indicator of a jump component lies in the slope of the term decay plot for OTM options as the option maturity falls within a month or so. A jump component exists if the term decay plot flattens out (slope approaching zero) as maturity nears.

Figure 5 depicts the two typical shapes of the term decay plots for S&P 500 index options on April 9, 1999 (the left panel) and on May 3, 2000 (the right panel). The plots follow the same convention as in the simulations (Figures 1, 2, and 4). They represent the two extreme cases that are experienced over the whole sample period. The term decay plots on April 9, 1999 (left panel) match the shapes generated from a purely continuous process: While the ATM term decay plot looks like a straight line, the OTM term decay plots exhibit strong concavity and positive slopes at short maturities. The short maturity slope estimates (at $\ln T = -4$) are, from top to bottom, $-0.377$, 1.670, 2.458, and 3.725, and the curvature estimates, $-0.027$, $-0.574$, $-0.783$, and $-1.100$, corresponding to moneyness levels of $k = 0$, $-3.07\%$, $-6.14\%$, and $-9.20\%$, respectively. The strongly negative curvature estimates and strongly positive short-maturity slope estimates for OTM options are indicative of an asymptotic $O(e^{-1/T})$ decay rate. Hence, the term decay plots on April 9, 1999 (left panel) reveal little sign of a jump component.

In contrast, the impacts of a jump component are vividly shown in the term decay plots on May 3, 2000 (right panel). The OTM term decay plots obviously

flatten out at short maturities. The short maturity slope estimates are, from top to bottom, $-0.604$, $-0.300$, $-0.116$, and 0.133, corresponding to moneyness levels of $k=0$, $-3.07\%$, $-6.14\%$, and $-9.20\%$, respectively. While the ATM term decay plot is strongly negatively sloped, the OTM plots all have short-maturity slopes close to zero. The curvature estimates for the four term decay plots are all very small, from $-0.07$ to 0.01.

On other days, the term decay plots fall between the two extreme cases. Figure 6 illustrates the different shapes of the term decay plots for ATM options (left panel) and for OTM options (right panel, $k=-9.2\%$). Most of the term decay plots for ATM options are strongly negatively sloped, indicating the dominance of an infinite variation component. Furthermore, the majority of the plots for OTM options exhibit some concavity and slightly positive slope at short maturities, indicating the existence of a jump component, possibly interacting with a continuous component. Overall, the existence of a jump component in the movement of S&P 500 index levels seems to vary significantly over time. Sometimes, its presence is strongly felt in the options market, while at other times its impact is almost nonexistent.

### *C. Is There a Continuous Component?*

When a continuous martingale component is present, the infinite variation required of it can have a strong impact on the term behavior of ATM option premia. When only a continuous martingale component is present, the term decay plots of ATM options are straight lines with an asymptotic slope of $-0.5$. However, since this behavior can also be generated by an infinite variation pure jump component, we need to interpret the term decay plots for ATM options with care. Nevertheless, various pieces of evidence suggest the existence of a continuous martingale component in the S&P 500 index movement.

The first piece of evidence comes from the term decay plots for ATM options in the left panel of Figure 6. Most of the plots are strongly negatively sloped and look like straight lines. This is strong evidence on the presence of an infinite variation component, which can be either a continuous martingale or an infinite variation pure jump process.

The second piece of evidence comes from days such as April 9, 1999 (left panel, Figure 5), when the presence of a jump component can hardly be detected. For such days, while we cannot identify the presence of a jump component from the OTM options, the presence of an infinite variation component is obvious in the ATM options premia. If there does not exist a jump component, the infinite variation component must be a purely continuous process.

Combining the two pieces of evidence together, we conclude that while the presence of a jump component is varying strongly over time, the continuous component has a more steady presence in the options data.

### *D. Time Varying Term Decay and Stochastic Volatility*

Figures 5 and 6 indicate that the daily term decay plots can take on very different shapes. It is important to understand whether such daily variations come

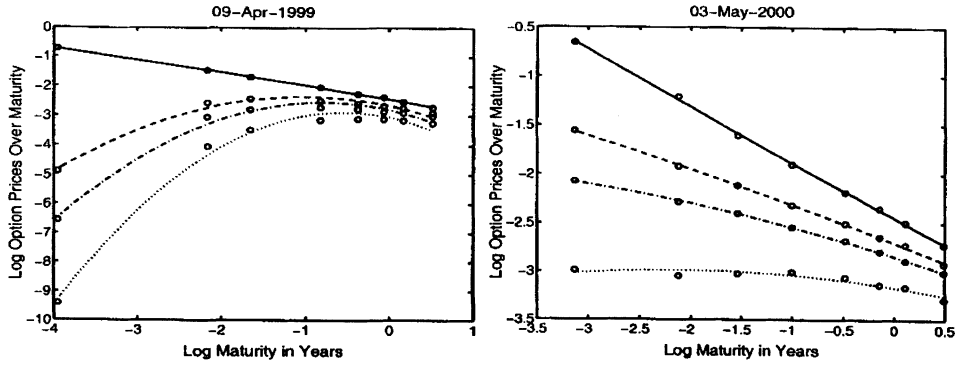


**Figure 5. Typical term decay plots for S&P 500 index options.** Circles represent data while lines represent second-order polynomial fits. The left panel depicts the term decay plots of S&P 500 index options on April 9, 1999. The right panel depicts that on May 3, 2000. In each panel, the four lines, from top to bottom, represent moneyness levels at $k = \ln K/F = 0$ (solid), $-3.07\%$ (dashed), $-6.14\%$ (dash-dotted), and $-9.20\%$ (dotted).

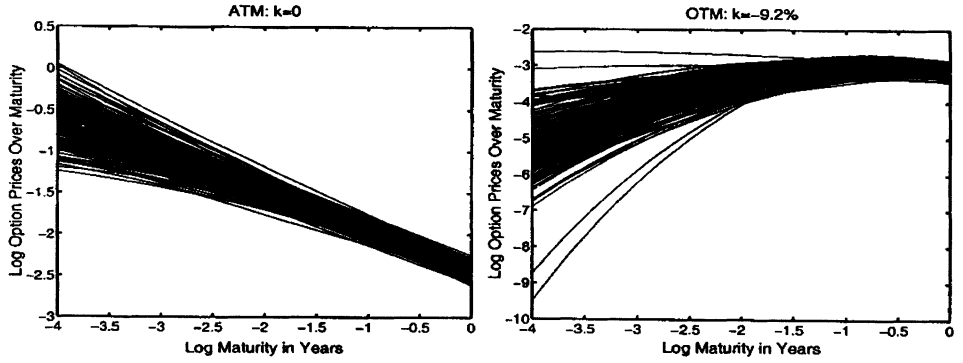


**Figure 6. Daily term decay plots for S&P 500 index options.** Lines represent smoothed daily term decay plots for S&P 500 index options from April 6, 1999 to May 31, 2000. The smoothing is performed based on second-order polynomial fits. The left panel depicts the term decay plots for ATM options ($k = 0$). The right panel depicts the term decay plots for OTM options with $k = -9.2\%$.

from data noise (e.g., microstructure effects) or underlie some fundamental movement in the underlying index process. We investigate this issue by analyzing the time-series properties of the term decay plots.

Figure 7 draws the time-series plots for the slope (left panel) and curvature (right panel) estimates on the term decay plots for both ATM options and OTM options ($\ln(K/F) = -9.2\%$). We observe that for ATM options (solid lines), the short-maturity slope estimates (left panel) fluctuate around $-0.5$ while the curvature estimates (right panel) fluctuate around 0. Thus, the term decay plots for ATM options exhibit relatively stable shapes over time: They are approximately linear lines with slope estimates around $-0.5$. Therefore, the presence of an infinite variation component is strongly and constantly felt.

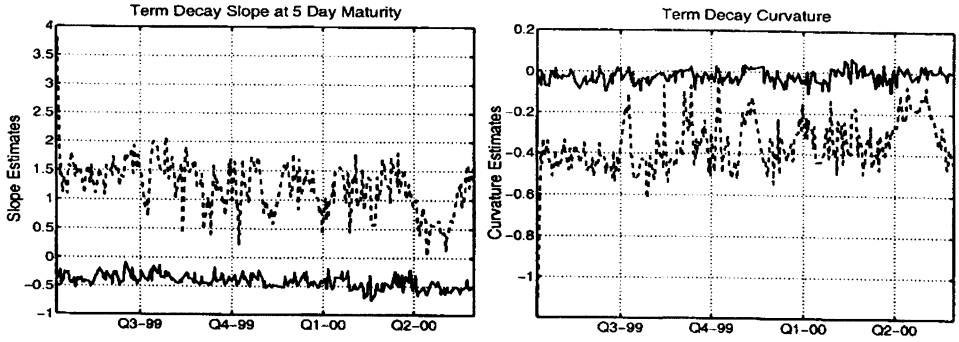


**Figure 7. The slope and curvature of the term decay plots for S&P 500 index options.** Lines in the left panel are the time series slope estimates of the term decay plots at 5 business day maturity while lines in the right panel are the time series of curvature estimates of the term decay plots. The estimates are based on a quadratic polynomial fit of the data at each day and moneyness. The solid lines represent the estimates on ATM term decay plots ($k = 0$) while the dashed lines are estimates for OTM plots ($k = -9.20\%$).

On the other hand, the slope and curvature estimates for the OTM term decay plots (dashed lines) are much more volatile. In particular, during the first two days (April 8 and 9, 1999) of the sample, the OTM term decay plots exhibit strongly positive slopes and strongly negative curvatures, indicating that option prices are approaching zero at a rate much faster than $O(T)$. The decay rate is more in line with $O(e^{-1/T})$, which is the rate implied by a purely continuous process. Indeed, the slope and curvature estimates are so large in magnitude and so far away from the majority estimates of the whole sample that they look like outliers. But further inspection of the data indicates that they are not outliers, but robust data points. In particular, we also find that, during the first 2 days of our sample, the implied volatility curves at short maturities are essentially flat. Only at relatively long maturities does a skewed pattern in volatility show up. This is consistent with the implication of pure continuous models with stochastic volatilities, for example, Heston (1993), but not with models with a significant presence of a jump component.

Nevertheless, the presence of a jump component is evident in the following days, as the slope estimates become much smaller, although still positive. The curvature estimates also become much less negative. When we move closer to April 2000, both the slope and the curvature estimates of the OTM term decay plots move very close to zero, implying that the jump component begins to dominate. Furthermore, the temporal patterns of the slope and curvature estimates indicate that the variations are not totally due to purely random noise such as measurement errors, but are indicative of systematic variation in the underlying, such as the presence of stochastic volatility.

Table III reports the summary statistics of these slope and curvature estimates. For ATM options, the sample average of the slope estimates is $-0.413$, slightly lower than implied by a continuous component. The sample average of the curvature is $-0.021$, very close to 0 and hence confirming the observation of

**Table III**

**Slope and Curvature of the Term Decay Plots on S&P 500 Index Options**

Entries report the summary statistics on the slope and curvature estimates from the smoothed term decay plots on S&P 500 index options. The smoothing is based on a second-order polynomial fit,

$$\ln(P/T) = a(\ln T)^2 + b(\ln T) + c,$$

where $P$ and $T$ denote, respectively, the put option price (as percentages of the underlying forward price level) and the maturity of the option. Based on the estimates for the polynomial coefficients, the slope of the term decay plot is $2a \ln T + b$ and the curvature, $2a$. We evaluate the slope at the short end of the maturity: $\ln T = -4$. The data are daily from April 6, 1999 to May 31, 2000, 273 business days. The statistics "Mean, Std, Auto, Skewness, Kurtosis" denote, respectively, the sample average, standard deviation, first-order autocorrelation, skewness, and excess kurtosis of the estimates. The last row, *Corr* ( · , *IV*), measures the correlations of these slope and curvature estimates with the fitted ATM implied volatility at short maturity ($\ln T = -4$).

| | $\ln K/F = 0$ | | $\ln K/F = -9.2\%$ | |
|---|---|---|---|---|
| Stats | Slope | Curvature | Slope | Curvature |
| Mean | −0.413 | −0.021 | 1.266 | −0.366 |
| Std | 0.114 | 0.032 | 0.441 | 0.128 |
| Auto | 0.506 | 0.422 | 0.586 | 0.559 |
| Skewness | 0.131 | −0.199 | 0.569 | −0.484 |
| Kurtosis | −0.102 | −0.293 | 4.846 | 4.598 |
| *Corr*( · , *IV*) | −0.749 | 0.540 | −0.584 | 0.515 |

negatively sloped near-straight lines. For OTM options at $\ln(K/F) = -9.2\%$, the average slope estimate is 1.266, and the average curvature estimate is −0.366, showing the combined effect of both a jump component and a continuous component. Furthermore, consistent with the observation from the time-series plots, the slope and curvature estimates for the OTM plots are much more volatile than that for the ATM plots. Nevertheless, these fluctuations are not purely random noise, but show significant persistence, as indicated by the first-order autocorrelations (from 0.422 to 0.589) on the slope and curvature estimates.

The systematic variation of the slope and curvature estimates for the term decay plots points to the presence of stochastic volatility. Nevertheless, depending upon the exact specification, stochastic volatility can generate different types of variations in the term decay plots. First, given a stationary volatility process, a shock to the volatility level has a larger impact on the short-term options than on the long-term options. Thus, with an increase in volatility, short-term option prices increase more than long-term option prices. The effects on the term decay plot are threefold: (1) the overall term decay plot shifts upward; (2) the short-maturity slope of the plot declines, that is, it becomes less positive or more negative; and (3) the concavity of the plot declines. Thus, holding everything else constant, these three effects will generate a negative correlation between the volatility level and the slope estimate and a positive correlation between volatility and the curvature of the term decay plot. Since all these three effects are a result of the overall volatility level change, we label them as the *volatility level effect.*

Furthermore, stochastic volatility not only alters the overall volatility level of an asset return, but also varies the *relative composition* of its components, say, a jump component and a purely continuous component. The variation of the relative composition of these two components will have yet another impact on the term decay plot. For example, when the volatility level increases, if the relative component of the jump component declines, two opposite effects will be imposed on the slope of the term decay plot for OTM options. On the one hand, the volatility level increase raises the short end of the term decay plot and makes the slope of the plot less positive. On the other hand, the decline in the jump component makes the diffusion component dominate and, hence, the slope of the OTM plot becomes more positive. Obviously, such an effect can reduce or even nullify the negative correlation between the volatility level and the slope of the OTM term decay plots. In contrast, these conflicting impacts will not be observed in the ATM term decay plots because increasing the volatility level and increasing the relative composition of the diffusion component both make the ATM term decay plot more negatively sloped. The correlation between the volatility level and the ATM term decay slopes shall become even more negative.

The jump-diffusion and stochastic volatility model applied in Bakshi et al. (1997) and Bates (1996) falls within this category. The model incorporates three components into the underlying price process: jumps (MJ), diffusion, and stochastic volatility. In both papers, stochastic volatility is generated through the instantaneous variance of the diffusion component, $v_t$, which is allowed to follow the square root process of Heston (1993). The arrival rate ($\lambda$) of the Poisson jump component, however, is assumed to be constant over time. Therefore, under this specification, as $v_t$ increases, the relative composition of the jump component declines. Thus, the impact of the instantaneous volatility level on the slope and curvature of the term decay plot would be a combined result of both the level effect and the composition effect.

We illustrate this delicate balancing effect by simulating this model. The model parameters are adopted from Carr and Wu (2003a), who calibrate the model to the same set of S&P 500 index options as used in this paper. The simulation results are summarized in Figure 8, where we plot the slope (left panel) and curvature (right panel) of the simulated term decay plots against the instantaneous variance level. As before, we first fit the term decay plot with a second-order polynomial and then compute the slope and curvature from this fitted curve. The slope is measured at $\ln T = -4$, while the curvature is global. The instantaneous variance on the $x$-axis is measured in terms of its log deviation from its mean level $v_t/\mathbb{E}[v]$. The circle-solid lines are estimates from the term decay plots of OTM options at moneyness $\ln(K/F) = -9.2\%$, while the diamond-dashed lines are for ATM options. We observe that the term decay plot slope for OTM options is highly nonlinear in the variance level. As long as $v_t/\mathbb{E}[v] > -0.5$, the level effect dominates and the slope declines as the variance increases. However, when the variance level is very low ($v_t/\mathbb{E}[v]$ less than $-0.5$), the composition effect begins to dominate. The slope of the relation becomes positive. A similar nonlinear relationship holds for the curvature of the OTM option term decay plots. In contract, since both the level and composition effects are in the same direction for ATM option

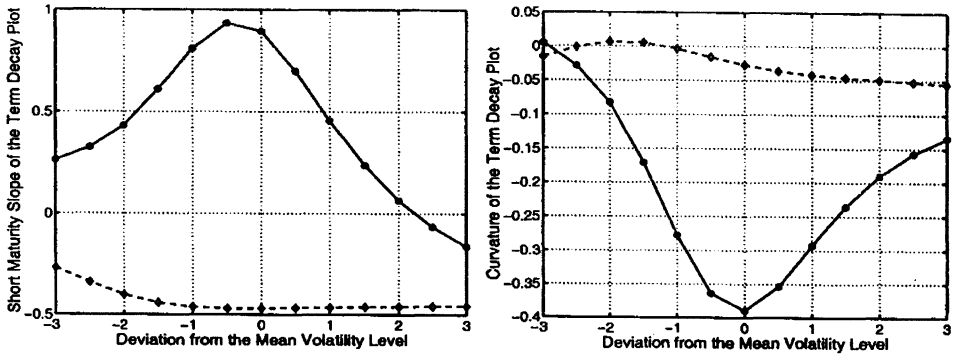


**Figure 8. Term decay plots under a jump-diffusion-stochastic volatility model.** Circle-solid lines are slope (left panel) and curvature (right panel) estimates of the term decay plots for OTM options at moneyness $\ln(K/F) = -9.2\%$. Diamond-dashed lines are for ATM options. The deviation from the mean volatility level is computed as $\ln v_t/\mathbb{E}[v]$. The plots are based on simulations of the jump-diffusion-stochastic volatility model of Bates (1996), with model parameters adopted from Carr and Wu (2002a). Short maturity slope at $\ln T = -4$ and curvature are estimated based on the second-order polynomial fitting of the term decay plot.

term decay plots, the ATM term decay slope is monotonically declining in the instantaneous variance (see the diamond-dashed line in the left panel of Figure 8).

For comparison, we plot the analogous relations for the S&P 500 index data in Figure 9. We use the ATM-implied volatility at the short maturity ($\ln T = -4$) as a proxy for the instantaneous volatility level. ATM implied volatility at each maturity is obtained via spline interpolation across moneyness. We then estimate the short maturity implied volatility through a second-order polynomial fit of the ATM implied volatilities ($IV$) across log maturities ($\ln T$),

$$IV = a(\ln T)^2 + b(\ln T) + c.$$

The fit performs reasonably well with an average $R$-squared of 0.92. At first glance, Figure 9 for the S&P 500 index options looks quite different from the graphs of the Bates (1996) model in Figure 8. In particular, the relations for the OTM S&P 500 index options data do not exhibit the strong nonlinearity observed in the simulated graphs. Nevertheless, a careful investigation of the simulated graphs indicates that the nonlinearities in the term decay plot slopes appear only when the volatility level is very low, when $\ln v_t/\mathbb{E}[v] < -0.5$. In practice, however, we observe very few data points with such low implied volatility. Within the range of observed implied volatility levels, the negative relation between the slope of the OTM term decay plots and the volatility level qualitatively matches those observed from the graphs of the Bates model.

In the last row of Table III, we report the correlations of the slope and curvature estimates of the term decay plots with the volatility level. The correlations between the volatility level and the term decay slopes are strongly negative, while that with the curvature are strongly positive. Furthermore, the negative

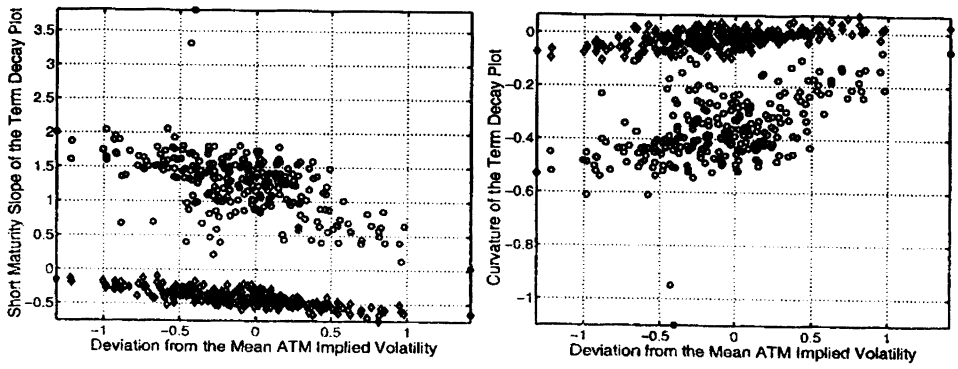


**Figure 9. The slope and curvature of the term decay plots for S&P 500 index options.** Circles are slope (left panel) and curvature (right panel) estimates of the term decay plots for OTM options at moneyness $\ln(K/F) = -9.2\%$. Diamonds are for ATM options. The deviation from the mean volatility level is computed as $\ln(IV_t^2/\overline{IV^2})$, where $IV_t$ is the fitted ATM implied volatility at short maturity ($\ln T = -4$) and $\overline{IV^2}$ denotes the sample average of this implied volatility squared. Short maturity slope at $\ln T = -4$ and curvature are estimated based on the second-order polynomial fitting of the term decay plot.

correlations between volatility and slopes are stronger for ATM options than for OTM options. This evidence is broadly consistent with the specification in Bakshi et al. (1997) and Bates (1996).

More recently, Bates (2000) and Pan (2002), among others, allow the arrival rate of the Poisson process to be an affine function of the instantaneous variance of the diffusion component: $\lambda_t = a + bv_t, a, b \in \mathbb{R}^+$ and, hence, the arrival rate of the Poisson jump is also allowed to be stochastic. Depending on the magnitude of the loading $b$ on the volatility factor, this model can generate either positive or negative correlations between the volatility level and the relative composition of the jump component. Thus, the model is even more flexible in generating the correlations observed in the data.

Nevertheless, under all of these specifications, the continuous component can totally disappear as $v_t \to 0$, while the jump component has a constant presence. In the former case, the jump intensity $\lambda$ is constant over time; in the latter case, the intensity has a constant component, $a$. The evidence on the term decay plots, however, seems to argue the other way around: While we do observe the jump component disappearing on some days, the presence of a continuous component is constantly felt. Thus, for model design, it seems that a simple role reversal would better capture the evidence from our term decay plots. That is, one can let the arrival rate of the Poisson jump component, $\lambda_t$, follow a mean reverting square root process, while the instantaneous variance of the diffusion component can be specified as an affine function of the Poisson intensity: $V_t = a + b\lambda_t, a, b \in \mathbb{R}^+$. This role reversal implies that while the arrival rate of the Poisson process can disappear, the diffusion component always has a constant presence.

Of course, there is no reason that the arrival rate of the jump component and the instantaneous variance of the diffusion component should be driven by the

same stochastic process. They may very well be driven by separate stochastic forces. Such a specification would also accommodate our evidence and could potentially generate better performance for option pricing. Most recently, Huang and Wu (2003) perform specification analysis on option pricing models based on time-changed Lévy processes (Carr and Wu (2003b)). They compare the empirical performance of different jump and stochastic volatility specifications in pricing S&P 500 index options. Consistent with our evidence in this paper, they find that allowing stochastic volatility to be generated separately from the jump component and the diffusion component significantly improves the pricing performance over traditional specifications.

## IV. Concluding Remarks

We provide a simple robust method to study the nature of the price process of an asset underlying an option. In particular, we map the short-maturity behavior of option prices to the type of process that the underlying asset price follows. Our analysis of S&P 500 index options indicates that there are both continuous and jump components in the underlying index process. Furthermore, we find that while the presence of the jump component varies strongly over time, the presence of the continuous component is constantly felt. These observations have interesting implications for specifications of the underlying price process, which can be further explored in future research.

## REFERENCES

Aït-Sahalia, Yacine, 2002, Telling from discrete data whether the underlying continuous-time model is a diffusion, *Journal of Finance* 57, 2075–2112.

Andersen, Leif, and Jesper Andreasen, 1999, Jumping smiles, *Risk*, November, 65–68.

Bakshi, Gurdip, Charles Cao, and Zhiwu Chen, 1997, Empirical performance of alternative option pricing models, *Journal of Finance* 52, 2003–2049.

Bates, David, 1996, Jumps and stochastic volatility: Exchange rate processes implicit in Deutsche Mark options, *Review of Financial Studies* 9, 69–107.

Bates, David, 2000, Post-'87 crash fears in the S&P 500 futures option market, *Journal of Econometrics* 94, 181–238.

Bertoin, Jean, 1996, *Lévy Processes* (Cambridge University Press, Cambridge, UK).

Black, Fisher, and Myron Scholes, 1973, The pricing of options and corporate liabilities, *Journal of Political Economy* 81, 637–654.

Brenner, Michael, and Marti Subrahmanyam, 1988, A simple formula to compute the implied standard deviation, *Financial Analysts Journal* 44, 80–83.

Carr, Peter, and Dilip Madan, 1999, Option valuation using the fast fourier transform, *Journal of Computational Finance* 2, 61–73.

Carr, Peter, and Liuren Wu, 2003a, Finite moment log stable process and option pricing, *Journal of Finance* 58, 753–777.

Carr, Peter, and Liuren Wu, 2003b, Time-changed Lévy processes and option pricing, *Journal of Financial Economics*, forthcoming.

Ding, Zhuanxin, and Clive W. J. Granger, 1996, Modeling volatility persistence of speculative returns: A new approach, *Journal of Econometrics* 73, 185–215.

Heston, Stephen, 1993, Closed-form solution for options with stochastic volatility, with application to bond and currency options, *Review of Financial Studies* 6, 327–343.

Huang, Jingzhi, and Liuren Wu, 2003, Specification analysis of option pricing models based on time-changed Lévy processes, *Journal of Finance*, forthcoming.

Jacod, Jean, and Albert N. Shiryaev, 1987, *Limit Theorems for Stochastic Processes* (Springer-Verlag, Berlin).

Merton, Robert C., 1976, Option pricing when underlying stock returns are discontinuous, *Journal of Financial Economics* 3, 125–144.

Pan, Jun, 2002, The jump-risk premia implicit in options: Evidence from an integrated time-series study, *Journal of Financial Economics* 63, 3–50.

Prokhorov, Yurii Vasilevich, and Albert Nikolaevich Shiryaev, 1998, *Probability Theory III: Stochastic Calculus* (Springer-Verlag, Berlin).

Protter, Philip, 1990, *Stochastic Integration and Differential Equations: A New Approach* (Springer, Berlin).

Varadhan, S. R. S., 1967, On the behavior of the fundamental solution of the heat equation with variable coefficients, *Communications in Pure and Applied Mathematics* 20, 431–455.